

Theory of multiparticle tunneling in diffusive superconducting junctions

E. V. Bezuglyi,^{1,2} A. S. Vasenko,^{1,3} E. N. Bratus',² V. S. Shumeiko,¹ and G. Wendin¹

¹*Chalmers University of Technology, S-41296 Göteborg, Sweden*

²*Institute for Low Temperature Physics and Engineering, Kharkov 61103, Ukraine*

³*Department of Physics, Moscow State University, Moscow 119992, Russia*

(Dated: February 8, 2020)

We formulate a theoretical framework to describe multiparticle current transport in planar superconducting tunnel junctions with diffusive electrodes. The approach is based on direct solving of quasiclassical Keldysh-Green function equations for nonequilibrium superconductors, and consists of a combination of a circuit theory analysis and improved perturbation expansion. The theory predicts much greater scaling parameter for the subharmonic gap structure of the tunnel current in diffusive junctions compared to the one in ballistic junctions and mesoscopic constrictions.

PACS numbers: 74.45.+c, 74.40.+k, 74.25.Fy, 74.50.+r.

I. INTRODUCTION

Multiparticle tunneling (MPT) is known to be a mechanism of dissipative current transport in superconducting tunnel junctions at the subgap applied voltage $eV < 2\Delta$, and at small temperature $T \ll \Delta$.^{1,2} The MPT refers to the tunneling regime of the multiple Andreev reflection (MAR),^{2,3,4,5} and it manifests itself in the set of the current steps at $eV = 2\Delta/n$ (n is an integer) – the subharmonic gap structure (SGS). Such structure is commonly observed in tunnel junctions with high-quality tunnel barriers,^{6,7,8,9} and in tunable mesoscopic constrictions in the tunneling regime.^{10,11,12} The theory predicts the scaling $\approx (D/2)^n$ for the tunneling SGS, where D is the bare transparency of the junction tunnel barrier.^{1,2,5} However, in the experiment, the SGS scaling parameter is generally much larger. A common explanation for this enhancement is the imperfection of the junction insulating layer.^{3,13} In Ref. 14 the attention was drawn to an alternative explanation: effect of disorder in planar junction electrodes; it was predicted that the SGS scaling parameter for planar diffusive junctions is enhanced by a factor $\sim \xi_0/\ell$, or even $\sim \xi_0^2/\ell d$ depending on the junction geometry (ξ_0 is the coherence length, ℓ is the elastic mean free path, d is the thickness of electrodes). In planar Al junctions with $\ell \sim d = 50$ nm and $\xi_0 = 300$ nm, the enhancement factor may approach the value 100.

In this paper we present a detailed theory of the MPT in planar Josephson tunnel junctions with diffusive thin-film electrodes. The theory is based on the direct solving of the Keldysh-Green's function equations of nonequilibrium superconductivity.¹⁵ The main technical difficulty with this approach is related to essentially nonstationary character of the Josephson tunnel transport. While analytical and numerical methods are well developed for solving stationary Usadel equation^{16,17} and nonequilibrium Keldysh-Usadel equation,¹⁸ the nonstationary problem was so far studied only numerically.¹⁹

The central model assumption made in this paper and relevant for the tunnel regime concerns discrimination of nonzero harmonics of the Green's functions and the distribution function. This approximation turns the originally difficult problem into an analytically tractable one, and at the same time it captures all qualitative, and to large extent quantitative prop-

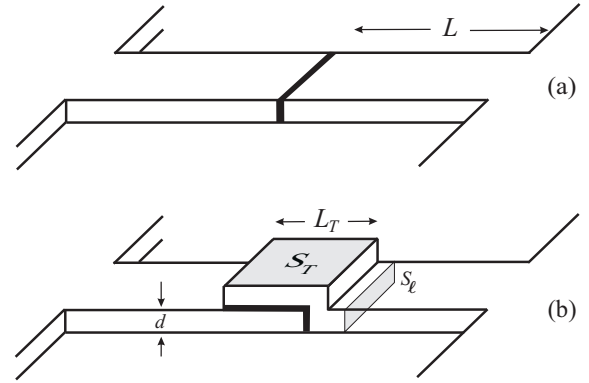


FIG. 1: One-dimensional (a) and planar (b) models of the tunnel junction.

erties of the tunneling SGS. Within this approximation we are able to develop a relatively simple and physically appealing calculation scheme, which combines the improved iterative procedure for evaluating the tunneling density of states (DOS), and the circuit theory methods for evaluating the spectral current.^{18,20}

The resulting physical picture of the MPT is as follows: The tunneling processes create the local DOS inside the bulk energy gap in the vicinity of the tunnel junction. This tunneling DOS allows quasiparticles to overcome the energy gap at a small applied voltage in several steps, by repeated bouncing between the junction electrodes (MAR). The spectral current through the energy gap, which determines the net charge current, is calculated by considering an effective circuit theory network representing the tunneling process. In this paper, we extensively discuss the relevant asymptotical methods and the details of the behavior of MPT currents.

The main practical result of the developed theory is a substantial enhancement of the SGS scaling factor.¹⁴ The effect can be qualitatively understood from a mesoscopic picture of the diffusive tunneling transport, namely, tunneling through a set of independent quasi-ballistic conducting channels with randomly distributed transparencies.^{20,21,22} Within this picture, the contribution of each channel can be evaluated using the ballistic MAR theory.^{2,4,5} In constrictions with length $L \gg \ell$ the transparencies are spread over the interval $\sim (L/\ell)D \gg D$,²³ which implies that the junction transpa-

rency, and hence the SGS scaling factor, are effectively enhanced by the factor L/ℓ . This explanation, however, is valid only for short constrictions, $L \ll \xi_0$, while it does not apply to planar tunnel junctions with lithographically fabricated overlapping thin-film electrodes commonly used in experiments and shown in Fig. 1. In these structures, massive pads (reservoirs) are fairly far from the junction ($L \gg \xi_0$); in such a situation the effective junction length is defined by the scale of spatial variation of the Green's function, i.e., by the coherence length. If the size L_T of the overlapping parts of the electrodes is comparable to the electrode thickness d , then the junction can be considered as an effectively one-dimensional (1D) one [see Fig. 1(a)]; in this case, the SGS enhancement factor becomes ξ_0/ℓ . If the junction cross-section is much larger than the cross-section of the electrodes [see Fig. 1(b)], the current concentrates not at the junction but rather in electrodes ("anti-constriction" geometry²⁴), and an additional enhancement factor ξ_0/d appears in the SGS scaling, which coincides with the result of rigorous calculation in this paper. Remarkably, this enhancement concerns only the multiparticle (Andreev) currents, while the single-particle current is not affected and is proportional to the bare barrier transparency D .^{25,26}

The fact that the SGS in planar junctions is sensitive to the properties of the junction electrodes has important implications for characterization of the junction tunneling layer. Indeed, the thickness of this layer in realistic junctions is non-homogeneous: there are spots with enhanced transparency, which mostly contribute to the tunnel current. If the linear sizes of such spots are large compared to the electron mean free path in the electrodes (in practice, the thickness of thin-film electrodes), the junction can be considered as a quasi-planar one, and the SGS should be enhanced according to our theory, and depend on the electrode thickness. However, if such spots are small compared to the electron mean free path, the tunnel current rapidly spreads out in immediate vicinity of the spot without being affected by the impurity scattering, as it is in the ballistic constrictions; in this case, there must be no dependence of the SGS on the electrode properties in accord with the mesoscopic theory prediction.^{2,4,5}

The paper is organized as follows. In its major part we develop a theory for the 1D junctions, Fig. 1(a), and discuss the extension to the planar junctions, Fig. 1(b), towards the end, in Sec. IV. We start with discussion of basic equations and adopted approximations in Sec. II. Then we construct the circuit theory in Sec. III, and develop a perturbation theory for the DOS in Sec. V. The MPT currents are calculated in Secs. VI and VII; the latter section includes also the calculation of the excess current. Effect of neglected harmonics in the Keldysh and Green's functions is evaluated in Sec. VIII.

II. 1D JUNCTION MODEL

A. Basic equations

The model of tunnel junction we are first going to study is depicted in Fig. 1(a) and consists of a tunnel barrier with the transparency D attached to bulk superconducting electrodes

via two superconducting leads ($-L < x < 0$ and $0 < x < L$). We will consider a diffusive limit, in which the elastic scattering length ℓ is much smaller than the coherence length $\xi_0 = \sqrt{\mathcal{D}/2\Delta}$, where \mathcal{D} is the diffusion coefficient (we assume $\hbar = k_B = 1$). The length L of the leads is assumed to be much larger than ξ_0 (long junction), and their width will be supposed to be much smaller than the Josephson penetration depth which implies homogeneity of the current along the junction. Similar model has been considered in Refs. 27 in study of the dc Josephson effect in tunnel structures.

Under these conditions, the microscopic calculation of the electric current $I(t)$ requires solution of the diffusive equations of nonequilibrium superconductivity¹⁵ (see also a review¹⁶) for the 4×4 matrix two-time Keldysh-Green's function $\check{G}(x, t_1, t_2)$ in the leads,

$$\begin{aligned} [\check{H}, \circ \check{G}] &= i\mathcal{D}\partial_x \check{J}, \quad \check{J} = \check{G} \circ \partial_x \check{G}, \quad \check{G} \circ \check{G} = \delta(t_1 - t_2), \quad (1) \\ \check{H} &= [i\sigma_z \partial_{t_1} - e\varphi + \hat{\Delta}(t_1)] \delta(t_1 - t_2), \end{aligned}$$

where $\hat{\Delta} = e^{i\sigma_z \phi} i\sigma_y \Delta$, φ is the electric potential, Δ and ϕ are the modulus and the phase of the order parameter, respectively, σ_i are the Pauli matrices, and

$$\check{G} = \begin{pmatrix} \hat{g}^R & \hat{G}^K \\ 0 & \hat{g}^A \end{pmatrix}, \quad \hat{G}^K = \hat{g}^R \circ \hat{f} - \hat{f} \circ \hat{g}^A. \quad (2)$$

In Eq. (2), $\hat{g}^{R,A}$ are the 2×2 Nambu matrix retarded and advanced Green's functions, and $\hat{f} = f + \sigma_z f_-$ is the matrix distribution function (we use 'check' for 4×4 and 'hat' for 2×2 matrices). The multiplication procedure in Eqs. (1) and (2) involves the time convolution

$$(A \circ B)(t_1, t_2) = \int_{-\infty}^{+\infty} A(t_1, t) B(t, t_2) dt.$$

In Eqs. (1) we neglect the inelastic collision term.

The boundary conditions for the function \check{G} and the matrix current \check{J} at the left ($x = -0$) and the right ($x = +0$) sides of the tunnel junction are given by relation²⁸

$$\check{J}_{-0} = \check{J}_{+0} = (2g_N R)^{-1} [\check{G}_{-0}, \circ \check{G}_{+0}], \quad (3)$$

where R is the junction resistance and g_N is the normal conductivity of the leads per unit length. The electric current is related to the Keldysh component of the matrix current \check{J} as $I(t) = (\pi g_N / 4e) \text{Tr} \sigma_z \hat{J}^K(x, t, t)$, and thus it can be expressed through the boundary value \check{J}_0 ,

$$I(t) = (\pi / 8eR) \text{Tr} \sigma_z [\check{G}_{-0}, \circ \check{G}_{+0}]^K(t, t). \quad (4)$$

Equations (1) can be decomposed into the diffusion equations for the Green's functions,

$$[\hat{H}, \circ \hat{g}] = i\mathcal{D}\partial_x \hat{J}, \quad \hat{J} = \hat{g} \circ \partial_x \hat{g}, \quad \hat{g} \circ \hat{g} = \delta(t_1 - t_2), \quad (5)$$

and the equation for the Keldysh component \hat{G}^K ,

$$[\hat{H}, \circ \hat{G}^K] = i\mathcal{D}\partial_x \hat{J}^K, \quad \hat{J}^K = \hat{g}^R \circ \partial_x \hat{G}^K + \hat{G}^K \circ \partial_x \hat{g}^A, \quad (6a)$$

$$\hat{g}^R \circ \hat{G}^K + \hat{G}^K \circ \hat{g}^A = 0. \quad (6b)$$

The boundary conditions for the functions \hat{g} and \hat{G}^K at the tunnel barrier follow from Eq. (3),

$$\hat{J}_0 = (W/\xi_0) [\hat{g}_{-0}, \circ \hat{g}_{+0}], \quad (7a)$$

$$\hat{f}_0^K = (W/\xi_0) [\check{G}_{-0}, \circ \check{G}_{+0}]^K. \quad (7b)$$

In Eqs. (7), the transparency parameter W is defined as

$$W = R(\xi_0)/2R = (3\xi_0/4\ell)D \gg D, \quad (8)$$

where $R(\xi_0) = \xi_0/g_N$ is the normal resistance of the piece of the lead with the length ξ_0 . It has been shown in Refs. 27 that it is this quantity rather than the barrier transparency D that plays the role of a true transparency parameter in the theory of diffusive tunnel junctions. In this paper, we will consider the limit $W \ll 1$, which corresponds to the conventional tunneling concept. In this case, according to Eqs. (7), the gradients of all functions are small. Within the tunnel model, which assumes the transparency parameter W to be the smallest parameter in the theory, these gradients are neglected, and the functions \hat{g} and \hat{f} are assumed to be local-equilibrium within the leads. In our consideration, we will lift this assumption and suppose the local-equilibrium form of these functions only within the bulk electrodes (reservoirs). Attributing the reference point for the phase, $\phi = 0$, to the left electrode, $x = -L$, these functions in the right electrode, $x = L$, are given by relations

$$\hat{g}(E, t) = \sigma_z u_S(E + \sigma_z eV) + ie^{i\sigma_z \phi(t)} \sigma_y v_S(E), \quad (9a)$$

$$(u_S, v_S) = (E, \Delta)/\xi, \quad \xi^{R,A} = [(E \pm i0)^2 - \Delta^2]^{1/2}, \quad (9b)$$

$$\hat{f}(E) = \tanh[(E + \sigma_z eV)/2T], \quad (9c)$$

written in terms of the mixed Wigner representation $A(E, t)$ of the two-time functions,

$$A(t_1, t_2) = \int_{-\infty}^{+\infty} \frac{dE}{2\pi} e^{-iE(t_1-t_2)} A(E, t). \quad (10)$$

In Eq. (10), the variable E has the meaning of the quasiparticle energy, and $t = (t_1 + t_2)/2$ is a real time. Similar equations, with $\phi = 0$ and $V = 0$, apply to the left electrode, $x = -L$.

Because of the small value of the tunneling parameter W one can neglect variations of the superconducting phase along the leads, as well as the charge imbalance function f_- proportional to a small electric field penetrating the superconducting leads. Furthermore, the small value of the superfluid momentum in the superconducting leads,²⁷ $p_s \sim W$, allows us to neglect a small effect of the suppression of the energy gap by the superfluid momentum²⁹ ($\sim p_s^{4/3} \sim W^{4/3}$). Within such an approximation, the coefficients in Eq. (1) at the left lead, $x < 0$, are time-independent functions. At $x > 0$, applying the gauge transformation³⁰ $\check{G}(t_1, t_2) = S^\dagger(t_1) \check{G}(t_1, t_2) S(t_2)$ with a unitary operator $S(t) = \exp[i\sigma_z \phi(t)/2]$ to the function \check{G} , we exclude the time-dependent phase and the electric potential from the equations for the function \check{G} and corresponding boundary conditions at $x = L$, which then become similar to the equations for $\check{G}(x)$ at $x < 0$ and the boundary conditions at $x = -L$. This results in the symmetry relation $\check{G}(x) = \check{G}(-x)$, which allows us to replace the function \check{G}_{+0} in the boundary condition

Eq. (3) and in the expression Eq. (4) for the electric current by the inverse gauge transformation of the function \check{G}_{-0} ,

$$\check{G}_{+0} \rightarrow \check{G}_{-0} \equiv S(t_1) \check{G}_{+0} S^\dagger(t_2) = S(t_1) \check{G}_{-0} S^\dagger(t_2).$$

As the result, the problem is reduced to the solution of a static equation within the left lead for the function $\check{G}(x, t_1, t_2)$, completed with the time-dependent boundary condition (3) at the tunnel barrier.³¹ It is convenient to expand all functions over harmonics of the Josephson frequency, $A(E, t) = \sum_m A(E, m) \exp(-2ieVmt)$, using the following rules for representation of the products and gauge-transformed values,

$$(A \circ B)(E, m) \quad (11)$$

$$= \sum_{m'} A[E + eV(m - m'), m'] B(E - eVm', m - m'),$$

$$\bar{A}(E, m) = \begin{pmatrix} A_{11}(E + eV, m), & A_{12}(E, m + 1) \\ A_{21}(E, m - 1), & A_{22}(E - eV, m) \end{pmatrix}. \quad (12)$$

In such a representation, the expression for the dc current I , Eq. (4), has the following form

$$I = \frac{1}{16eR} \int_{-\infty}^{\infty} dE \text{Tr}(\hat{h} \circ \bar{\check{G}}^K - \bar{\check{h}} \circ \check{G}^K)(E, 0) \quad (13)$$

$$= \frac{1}{16eR} \int_{-\infty}^{\infty} dE \text{Tr} \sum_m [\hat{h}(E, m) \bar{\check{G}}^K(E, -m) - \bar{\check{h}}(E, m) \check{G}^K(E, -m)], \quad \hat{h} = \sigma_z \hat{g}^R - \hat{g}^A \sigma_z.$$

In this formula all functions are taken at the boundary $x = -0$. We will adopt the same convention in the most of following equations and suppress the spatial coordinate assuming that it is taken at the boundary.

B. Zero-harmonic model

Solving a complicated system of nonlinear differential equations (5)–(7) is a very difficult task, which can be fulfilled only numerically even in the 1D case. The solutions can be constructed in the adiabatic limit of small applied voltage $eV \ll \Delta$.³² To make the problem tractable at larger voltages $eV \sim \Delta$, we make use of the observation that the amplitudes of high-order harmonics of the function \check{G} are small in the tunneling limit $W \ll 1$: the amplitude of the m th harmonic decreases with m as W^m . This suggests that zero harmonics $m = 0$ play the key role in Eq. (13), while the high-order harmonics are neglected. Thus we adopt an approximation scheme, in which only the zero harmonics of the functions \hat{g} and \hat{G}^K are kept. It turns out that such an approximation is sufficiently powerful to recover all specific features of the MPT currents, and to give qualitatively satisfactory description of the SGS of the net tunnel current. Furthermore, our analysis of the correction due to the first harmonics in Sec. VIII shows that the zero-harmonic model may give rather good quantitative agreement with the result of full numerical calculation.

For the matrix structure of the zero harmonic of the function \hat{g} in Eq. (13), we adopt the approximation

$$\hat{g}(E, 0) = \sigma_z u(E) + i\sigma_y v(E), \quad u^2 - v^2 = 1, \quad (14)$$

which is similar to the Green's function structure in the left electrode [see Eqs. (9)], though u and v have a different form. It is possible to prove, using the normalization condition in Eq. (5), that the zero harmonic of matrix \hat{g} is traceless, and that the σ_x -component of this matrix is much smaller in the tunneling limit (at least by W^2) than the "main" components u and v , which have zero order in the parameter W . Within the same approximation, the Keldysh function \hat{G}^K has the form

$$\hat{G}^K(E, 0) = 2f(E)[\sigma_z N(E) + i\sigma_y M(E)], \quad (15)$$

where $N(E) = \text{Re } u^R$ is the density of states (DOS) normalized to its value in the normal state and $M(E) = \text{Re } v^R$. Furthermore, we will express the advanced Green's functions through the retarded ones, $(u, v)^A = -(u, v)^{R*}$, using the general relation $\hat{g}^A = -\sigma_z \hat{g}^{R\dagger} \sigma_z$, and omit the superscript R , assuming all Green's functions to be retarded.

Retaining only zero harmonics of the Green's functions \hat{g} and \hat{G}^K in Eq. (13), we find that only the *diagonal* parts $h(E)$ and $G^K(E)$ of the corresponding matrices enter the dc current

$$I = \frac{1}{32eR} \int_{-\infty}^{\infty} dE \text{Tr} \sum_{k=\pm 1} (1 + k\sigma_z)[h(E)G^K(E + keV) - h(E + keV)G^K(E)]. \quad (16)$$

By introducing the distribution function $n = (1/2)(1 - f)$ that approaches the Fermi function n_F in equilibrium, Eq. (16) exactly transforms to the standard form for the tunnel current,

$$I = \frac{1}{eR} \int_{-\infty}^{\infty} dE n(E)N(E - eV)[n(E - eV) - n(E)], \quad (17)$$

with that essential difference that the DOS and the distribution function are not given, but are to be computed from the Keldysh-Green's function equations. To zero order in the tunneling parameter, the DOS has the BCS form $N_S(E) = \text{Re}(E/\xi^R)$, and the distribution function is the equilibrium one, $n = n_F$. In this approximation, Eq. (17) recovers the single-particle current of the tunnel model.²⁶ At zero temperature this current acquires the form

$$I = \frac{1}{eR} \int_{\Delta}^{eV - \Delta} dE N_S(E)N_S(E - eV), \quad (18)$$

and turns to zero at $eV < 2\Delta$, having a sharp onset at $eV = 2\Delta$, $I_1(2\Delta) = \pi\Delta/2eR$.

To calculate the current at smaller, subgap voltages $eV < 2\Delta$, one has to calculate the tunneling corrections to the BCS DOS, and to find the nonequilibrium distribution function.

III. CIRCUIT REPRESENTATION OF BOUNDARY CONDITION

We start with evaluation of the distribution function, and develop a circuit theory approach to derive a general analytical equation for the current in Eq. (17) assuming the DOS to be modified in a close vicinity of the tunnel barrier.

A. Kinetic equation and boundary condition

Using zero harmonic of Eqs. (6a) and (7b), we obtain the diffusive kinetic equation and the boundary condition

$$\partial_x (D_+ \partial_x n) = 0, \quad (19a)$$

$$D_+ \partial_x n|_{x=0} = (2W/\xi_0) \sum_{k=\pm 1} NN_k (n_k - n)|_{x=0}, \quad (19b)$$

where $D_+ = (1/2)(1 + |u|^2 - |v|^2)$ is the dimensionless diffusion coefficient. The subscript k denotes the energy shift: $n_k(E) \equiv n(E_k) = n(E + keV)$.

It follows from Eq. (19a) that $D_+ \partial_x n = \text{const}$; this constant value can be found from Eq. (19b). At $x \gg \xi_0$ the coefficient D_+ approaches the BCS form $D_S = \Theta(|E| - \Delta)$ [$\Theta(x)$ is the Heaviside step function] and exactly turns to D_S at the reservoir, $x = -L$. This implies that at subgap energies $|E| < \Delta$, the quasiparticle probability current $D_+ \partial_x n$ turns to zero along the whole lead, and the distribution function is spatially homogeneous. Physically, this manifests complete Andreev reflection in terms of quasiparticle flows in diffusive structures.

Outside the gap, Eq. (19a) has no bound solutions: the distribution function grows linearly with x far from the junction. Such a growth is limited in practice by inelastic collisions, which provide relaxation of $n(x, E)$ to the equilibrium value n_F at the distance of inelastic scattering length l_e . To simplify the problem, we consider, instead of including a complicated inelastic collision term, a junction geometry with short enough leads having the length $L \ll l_e$ (but still $L \gg \xi_0$) and connected at $x = \pm L$ to equilibrium reservoirs. Within this model, the Green's functions, which change at $x \sim \xi_0$, are not affected by the finite length of the leads, while the reservoirs impose the equilibrium boundary conditions for the distribution function, $n(\pm L) = n_F$. At the same time we can neglect inelastic collisions inside the leads. Obviously, this model describes a qualitative pattern of inelastic relaxation in very long channel ($L \gg l_e$) with substitution $L \rightarrow l_e$ in our results.

Generally, spatial variation of $n(x)$ at $|E| > \Delta$ has two scales: linear x -dependence at $x \sim L$ and fast but small variations near the junction due to spatial dependence of the Green's function. The corresponding expansion of $n(x)$ over ξ_0/L at $x < 0$ reads

$$n(x) = n(0) + \frac{x}{L}[n(0) - n_F] \left[1 - \int_{-\infty}^0 \frac{dx}{L} d_+(x) \right] + [n(0) - n_F] \int_0^x \frac{dx'}{L} d_+(x'), \quad (20)$$

where the quantity $d_+(x) = D_+^{-1}(x) - 1$ describes small ($\sim W$) variations of the diffusion coefficient in the vicinity of the barrier and rapidly turns to zero at $x \gg \xi_0$. We will neglect these small corrections to the diffusion coefficient and, correspondingly, to the distribution function and use the relation $D_+ \partial_x n = [n(0) - n_F]L^{-1}$ following from Eq. (20) within the main approximation in the parameters W and ξ_0/L . Substituting this relation into the boundary condition (19b) and accounting for $D_+ \partial_x n = 0$ at $|E| < \Delta$, we obtain the equation

$$\Theta(|E| - \Delta)(n - n_F) = r \sum_{k=\pm 1} NN_k (n_k - n). \quad (21)$$

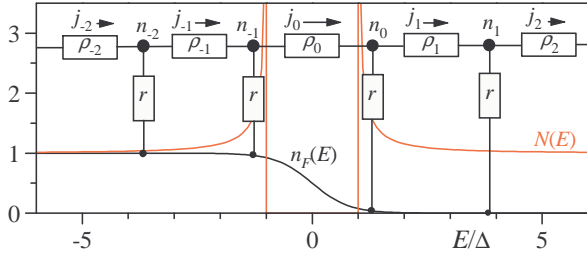


FIG. 2: (Color online) Circuit theory network with the period eV representing charge transport in diffusive tunnel junctions, $eV = 2.5\Delta$.

In this and following equations, the functions are taken at the boundary $x = -0$. Equation (21) represents a recurrence relation between the values of $n(E, 0)$ at the energies shifted by eV ; the nonequilibrium parameter r is defined as

$$r = 2LW/\xi_0 = R_N/R, \quad (22)$$

where $R_N = L/g_N$ is the normal resistance of one lead. In practice, the tunnel resistance much exceeds the resistance of the leads, $R \gg R_N$, and the nonequilibrium parameter is small, $r \ll 1$, which implies that at the energies $|E| > \Delta$, the distribution function is always close to the Fermi function.

B. Circuit theory

We split the integral in Eq. (17) into pieces of length eV ,

$$I = \frac{1}{eR} \int_{-\infty}^{\infty} dE j_0(E) = \frac{1}{eR} \int_0^{eV} dE J(E), \quad (23)$$

$$J = \sum_{k=-\infty}^{\infty} j_k, \quad j_k = (n_{k-1} - n_k) \rho_k^{-1}, \quad \rho_k^{-1} = N_k N_{k-1}.$$

In these notations the recurrence relation Eq. (21) reads

$$\Theta(|E_k| - \Delta) [n_k - n_F(E_k)] = r(j_k - j_{k+1}). \quad (24)$$

A convenient interpretation of Eqs. (23) and (24) in terms of the circuit theory¹⁸ is given by an infinite network in the energy space with the period eV , graphically presented in Fig. 2. The electric current spectral density $J(E)$ consists of partial currents j_k which flow through the chain of tunnel “resistors” ρ_k connected to adjacent nodes of the network having “potentials” n_k and n_{k-1} . At $|E| > \Delta$, the nodes are also attached to the distributed “equilibrium source” $n_F(E)$ through equal resistors r . In this representation the recurrence relation Eq. (24) has the meaning of “Kirchhoff’s rules” for partial currents.

Below we assume the equilibrium quasiparticle distribution $n(E) = n_F(E)$ at $|E| > \Delta$, neglecting effect of small resistors r . The role of nonequilibrium ($r \neq 0$) will be discussed elsewhere. In this limit, the currents j_k outside the energy gap, $|E_k| > \Delta$, vanish at zero temperature since n_F is piecewise constant. At $T \neq 0$, these currents describe the effect of thermal excitations. The subgap spectral current is conserved, $j_k = j_\Delta = \text{const}$, $k = 1 - N_-, \dots, N_+$ [as a consequence of Eq. (24)], and can be easily computed,

$$j_\Delta = [n_F(E_{-N_-}) - n_F(E_{N_+})] \rho_\Delta^{-1},$$

$$N_\pm(E) = \text{Int}[(\Delta \mp E)/eV] + 1, \quad \rho_\Delta(E) = \sum_{k=1-N_-}^{N_+} \rho_k,$$

where the integers $\pm N_\pm$ are the numbers of the nodes outside the gap nearest to the gap edges, $\text{Int}(x)$ denotes integer part of x , and the quantity $\rho_\Delta(E)$ has the meaning of the net subgap resistance. The subgap distribution function reads

$$n(E) = n_F(E_{N_+}) + [n_F(E_{-N_-}) - n_F(E_{N_+})] \sum_{k=1}^{N_+} \rho_k \rho_\Delta^{-1}. \quad (25)$$

The resulting electric current can be now written in a general form, for arbitrary voltages and temperatures,

$$I = \int_0^{eV} \frac{dE}{eR} (N_- + N_+) j_\Delta + 2 \int_\Delta^\infty \frac{dE}{eR} \frac{n_F(E) - n_F(E_1)}{\rho_1}. \quad (26)$$

Here the first term describes the subgap current, and the second term – the current of thermal excitations.

The magnitude of the subgap current is fully determined by the net subgap resistance; the current is blocked when this resistance is infinite, $\rho_\Delta = \infty$, which happens when DOS turns to zero. According to Eq. (26), the amount $N_- + N_+$ of the resistors contributing to the subgap resistance gives the amount of electric charge (in units of e) transferred during the tunneling event. Thus, the circuit with one subgap resistor represents the single-particle tunneling, which can exist only at $eV > 2\Delta$; in this case, Eq. (26) reduces to Eq. (18). At $eV < 2\Delta$, the subgap circuit should consist of at least two resistors (two-particle tunneling). However, for the BCS DOS this current is blocked, and to evaluate the current one has to calculate the tunneling correction to the DOS within the gap by solving the Green’s function equations.

IV. PLANAR JUNCTIONS

In this section we will discuss the extension of our approach to a more practical case of planar tunnel junction sketched in Fig. 1(b). This 2D case is more complex; however, it is possible to reduce this problem to the 1D case by formulating effective boundary conditions at the junction following the method suggested by Volkov.²⁴

Let us suppose that the size of the junction L_T exceeds the coherence length, $L_T \gg \xi_0$, and, simultaneously, does not exceed the Josephson penetration depth. Then the function \check{G} in the left-hand side (lhs) of the kinetic equation $[\check{H}, \circ\check{G}] = i\mathcal{D}\nabla\check{J}$ is approximately constant within the junction banks (parts of the junction leads of lengths L_T beneath and above the insulator). Then, integrating this equation over the volume of the bottom bank, using boundary conditions Eq. (3), and denoting the cross-section area of the lead as S_ℓ , the lead thickness as d , and the area of the junction as S_T , we obtain

$$S_T d [\check{H}, \circ\check{G}] = i\mathcal{D} \{ S_T (W/\xi_0) [\check{G}_{-0}, \circ\check{G}_{+0}] - S_\ell \check{J}_\ell \}, \text{ or}$$

$$[\check{H}, \circ\check{G}] = 2i\Delta \{ \tilde{W} [\check{G}_{-0}, \circ\check{G}_{+0}] - (\xi_0^2/L_T) \check{J}_\ell \}, \quad (27)$$

where ± 0 denotes top and bottom side of the barrier,

$$\tilde{W} = W(\xi_0/d) = (3\xi_0^2/4ld)D \quad (28)$$

is the effective tunneling parameter, and \check{J}_ℓ is the value of the matrix current at the lead cross-section adjoining the junction.

As soon as $\xi_0 \ll L_T$ and $\xi_0 \tilde{J}_\ell \sim W$, the last term in Eq. (27) can be assumed to be the smallest one and thus neglected. However, this is only true for the Green's component of Eq. (27),²⁴

$$[\check{H}, \circ \check{g}] = 2i\Delta \tilde{W} [\check{g}_{-0}, \circ \check{g}_{+0}], \quad (29)$$

whereas for the Keldysh component, the diagonal part of the lhs of Eq. (27) turns to zero (we consider only zero harmonics), and therefore the boundary condition for the diagonal part of \check{f}_ℓ^K , which is proportional to $D_+ \partial_x f$, has the form

$$\check{f}_\ell^K = (W_f / \xi_0) [\check{G}_{-0}, \circ \check{G}_{+0}]^K, \quad (30)$$

where $W_f = W(L_T/d) \gg \tilde{W}$. Equation (30) is the boundary condition for the distribution function, which is to be used as described above. Solving kinetic equation within the lead and assuming $L \gg L_T$, we arrive at the equation similar to Eq. (24) with the same parameter of nonequilibrium,

$$r = \frac{2W_f L}{\xi_0} = 2L \frac{R(\xi_0)}{2\xi_0 R} \frac{L_T}{d} = L \frac{\rho}{S_T R} \frac{L_T}{d} = \frac{L\rho}{S_\ell R} = \frac{R_N}{R},$$

where ρ is the specific conductivity of the leads, R_N is the resistance of one lead. Here we used the fact that the definition of $R(\xi_0) = \rho \xi_0 / S_T$, i.e., resistance of the leads (banks) per length ξ_0 which enters the definition of the bare $W = R(\xi_0) / 2R$, is related to the 1D geometry.

V. PERTURBATION THEORY FOR THE GREEN'S FUNCTIONS

To calculate the DOS within the next approximation with respect to the parameter W , we solve Usadel equation for the Green's function \hat{g} following from Eqs. (5). Introducing the parametrization $\hat{g} = \sigma_z \exp(\sigma_x \theta)$ via the spectral angle θ and the dimensionless coordinate z , we arrive at the equation

$$\sinh[\theta(z) - \theta_S] = i\theta''(z) \sinh \theta_S, \quad z = x/\xi_0, \quad (31)$$

where the prime sign denotes the derivative over z . With exponential accuracy, the solution of Eq. (31) at $z < 0$ can be approximated by the formula for a semi-infinite superconducting wire,³³

$$\tanh[(\theta(z) - \theta_S)/4] = \tanh[(\theta(-0) - \theta_S)/4] \exp(kz), \quad (32)$$

where $k^{-1}(E) = \sqrt{i \sinh \theta_S}$. Equation (32) describes the decay of perturbations of the spectral functions at distances $\gtrsim \xi_0$ from the barrier, where the spectral angle approaches its bulk value $\theta_S = \text{arctanh}(\Delta/E)$. The boundary condition for the spectral angle in the 1D geometry follows from Eq. (7a),

$$\theta' + W \sinh \theta (\cosh \theta_1 + \cosh \theta_{-1}) \Big|_{z=-0} = 0. \quad (33)$$

Then the boundary value of θ can be found from the finite-difference equation following from Eqs. (33) and (32),

$$2k \sinh[(\theta_S - \theta)/2] = W \sinh \theta (\cosh \theta_1 + \cosh \theta_{-1}). \quad (34)$$

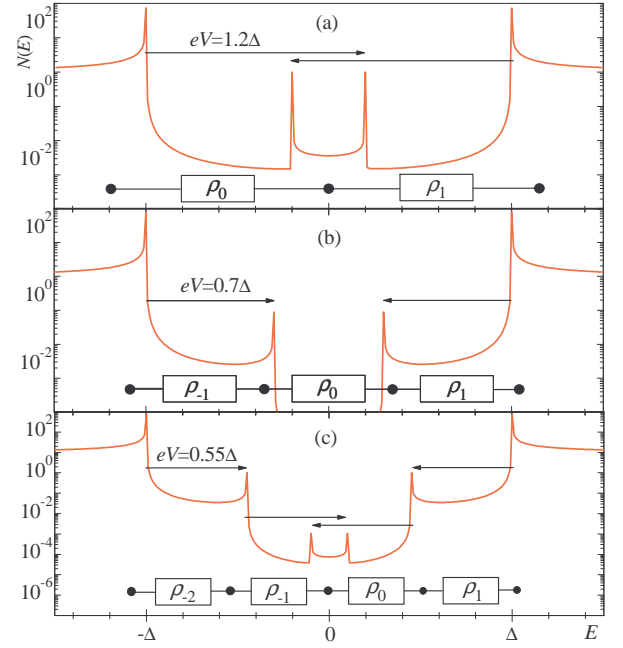


FIG. 3: (Color online) Numerically computed DOS and typical sub-gap circuits describing the two-particle current at $eV = 1.2\Delta$ (a), the three-particle current at $eV = 0.7\Delta$ (b), and the four-particle current at $eV = 0.55\Delta$ (c), for the tunneling parameter $W = 10^{-3}$.

A similar result can be obtained for the planar junction. Taking the x -component of Eq. (29), we arrive at the equation for the spectral angle in junction banks,

$$k^2 \sinh(\theta_S - \theta) = \tilde{W} \sinh \theta (\cosh \theta_1 + \cosh \theta_{-1}). \quad (35)$$

In what follows, we will discuss both of the junction geometries simultaneously, using common notation W for both transparency parameters W and \tilde{W} and assuming this quantity to be defined by Eq. (8) or Eq. (28) depending on the context.

A. Simple perturbation theory

Due to the presence of the small parameter W in the right-hand side (rhs) of equation Eq. (34), one can suggest the following perturbation correction for θ to first order in W ,

$$\theta = \theta_S - Wk^{-1} \sinh \theta_S [\cosh \theta_{S,1} + \cosh \theta_{S,-1}], \quad (36)$$

and similar for Eq. (35). This results in the following expression for the DOS $N(E) = \text{Re}(\cosh \theta)$ within the BCS gap,

$$\begin{aligned} N(E) &= W(1 - E^2/\Delta^2)^{-a/2} [N_S(E + eV) + N_S(E - eV)] = \\ &= W |\Delta/\xi|^{-a} (N_{S,1} + N_{S,-1}), \end{aligned} \quad (37)$$

$$|\xi| = \sqrt{\Delta^2 - E^2}, \quad a = \begin{cases} 5/2, & \text{1D junction;} \\ 3, & \text{planar junction.} \end{cases}$$

Such approximation will be referred to below as the result of a simple perturbation theory (SPT).

As follows from Eq. (37), the tunneling coupling extends the DOS inside the gap over the distance eV from the gap

edges, and scales it down by the factor W , as shown in Fig. 3. It is clear from Eq. (37) that with decreasing voltage, at $eV < \Delta$, the gap will open in the DOS [see Fig. 3(b)], and further iteration of the finite-difference equations (34) or (35) for the spectral angle will be required. As the result of this iterative scheme, the DOS at small enough eV acquires a staircase structure in the energy space: the two ladders descending from the bulk gap edges inside the subgap region; the height of n th step is W^n , and the width is eV . In the middle of the gap, $-\Delta + (n-1)eV < E < \Delta - (n-1)eV$ (assuming $eV < 2\Delta/n$), there is a plateau with the height $\approx 2W^n$ [see Fig. 3(a) and (c)]. While eV decreases, the plateau expands until its size becomes equal to $2eV$, then a new pair of steps emerges, which happens when n is even. We recall that this deformation of the DOS occurs only locally, at the distance $x \sim \xi_0$ from the junction.

B. Improved perturbation theory

The subgap DOS in Eq. (37) possesses singularities at the gap edges $|E| = \Delta$, which causes divergence of the subgap current at relatively large voltage, as we will see later. To eliminate the divergence, we need to apply an improved perturbation theory (IPT) to Eqs. (34) and (35), in which nonlinearity of the recurrence relations is fully taken into account. First, we consider approximation to Eq. (34), in which the non-singular terms $\cosh \theta_{\pm 1}$ are replaced with their BCS values, but we do not suppose that the difference $\theta - \theta_S$ is small,

$$\begin{aligned} \sinh[(\theta_S - \theta)/2] &= Wk^{-1} \sinh \theta g(E, eV), \\ g(E, eV) &= (1/2)(\cosh \theta_{S,1} + \cosh \theta_{S,-1}). \end{aligned} \quad (38)$$

In the vicinity of the point $E = \Delta$ the function $g(E, eV)$ is regular and thus can be approximated by $g(\Delta, eV)$ (it is sufficient to consider only positive values of E due to the symmetry of the spectral functions). Within the region $|E - \Delta| \ll \Delta$, the spectral angles $\theta(E)$ and $\theta_S(E)$ are large, therefore we hold only large exponents $\exp \theta$ and $\exp \theta_S$ in the hyperbolic functions in the rhs of Eq. (38), and use the asymptotic expression $\exp \theta_S \approx [2\Delta/(E - \Delta)]^{1/2}$. Then, introducing a dimensionless energy variable ε and a normalized spectral function $z(\varepsilon)$ as

$$\varepsilon = (\Delta - E)/2\Delta p^2, \quad p(eV) = [W^2 g^2(eV)/2]^{1/3}, \quad (39a)$$

$$z(\varepsilon) = ip \exp \theta, \quad \exp \theta_S = (ip\sqrt{\varepsilon})^{-1} \quad (39b)$$

we reduce Eq. (38) to a numerical algebraic equation

$$z^3 + (z\sqrt{\varepsilon} - 1)^2 = 0. \quad (40)$$

The relevant solution $z(\varepsilon)$ of Eq. (40) is determined by the requirement for the asymptotic behavior at $\varepsilon \gg 1$ to coincide with the energy dependence $z(\varepsilon) \approx \varepsilon^{-1/2} + i\varepsilon^{-5/4}$ given by the direct perturbative expansion Eq. (36). For planar geometry, we directly obtain the function $z(\varepsilon)$ and the scaling parameter p from Eq. (35),

$$z(\varepsilon) = (\varepsilon - i)^{-1/2}, \quad p(eV) = [Wg(eV)]^{1/2}. \quad (41)$$

The resulting DOS in the region $|E - \Delta| \ll \Delta$,

$$N(E, eV) = [2p(eV)]^{-1} \text{Im } z(\varepsilon), \quad (42)$$

approaches a finite value $N(\Delta, eV) \sim W^{-b}(eV - 2\Delta)^{-b/2}$ at $E = \Delta$, where

$$b = \begin{cases} 2/3, & \text{1D junction;} \\ 1/2, & \text{planar junction.} \end{cases} \quad (43)$$

However, in the vicinity of the specific voltage value $eV = 2\Delta$ the DOS diverges, and the calculation procedure must be further improved. The problem is caused by the fact that at $eV = 2\Delta$ both the energies E and $E - eV$ in Eqs. (34) or (35) approach the gap edges Δ and $-\Delta$, respectively. Therefore one must solve the equation not only for $N(E)$, but for $N(E - eV)$ as well. To this end we consider the recurrence Eq. (34) for two energies E and $E - eV$, and replace the non-singular terms $\cosh \theta_1$ and $\cosh \theta_{-2}$ by their BCS values,

$$\sinh \frac{\theta_S - \theta}{2} = \frac{W \sinh \theta}{2k} (\cosh \theta_{-1} + \cosh \theta_{S,1}), \quad (44a)$$

$$\sinh \frac{\theta_{S,-1} - \theta_{-1}}{2} = \frac{W \sinh \theta_{-1}}{2k_{-1}} (\cosh \theta_{S,-2} + \cosh \theta). \quad (44b)$$

Using again the fact that the spectral angles are large in the region $|E - \Delta| \ll \Delta$, we hold only large exponents $\exp \theta$, $\exp \theta_S$, and $\exp(-\theta_{-1})$, $\exp(-\theta_{S,-1})$ in the rhs of Eqs. (44), and use the asymptotic expressions $\exp \theta_S \approx [2\Delta/(E - \Delta)]^{1/2}$ and $\exp(-\theta_{S,-1}) \approx [2\Delta/(eV - \Delta - E)]^{1/2}$. Then, introducing dimensionless energy and voltage variables ε and Ω , and normalized spectral functions $z(\varepsilon)$ and $\bar{z}(\varepsilon)$,

$$\begin{aligned} \varepsilon &= (E - \Delta)/2\Delta q^2, & \Omega &= (eV - 2\Delta)/2\Delta q^2, \\ \exp \theta &= zq^{-1}, & \exp(-\theta_{-1}) &= \bar{z}q^{-1}, & q &= W^{2/5}/2. \end{aligned} \quad (45)$$

we obtain the equations for the functions $z(\varepsilon)$ and $\bar{z}(\varepsilon)$,

$$\begin{aligned} (1 - zR)^2 &= iz^3 \bar{z}^2, & (1 - \bar{z}R)^2 &= -i\bar{z}^3 z^2, \\ R(\varepsilon) &= \sqrt{\varepsilon + i0}, & \bar{R}(\varepsilon) &= R(\Omega - \varepsilon), \end{aligned}$$

which reduce to a single equation for the function $z(\varepsilon)$,

$$[z^3(1 - zR)^{-2} + i\bar{R}^2]^2 + iz[(1 - zR)^2 - 4z\bar{R}] = 0; \quad (46)$$

the function \bar{z} can be then found as $\bar{z} = (1 - zR)/\sqrt{iz^3}$. The relevant root of Eq. (46) is fixed by its asymptotic behavior far enough from the gap edge, at $|\varepsilon| \gg 1$, which can be independently calculated using the direct expansion Eq. (36). For planar geometry, we obtain the equations

$$(1 - z^2 R^2)^2 (z + i\bar{R}^2) + iz^4 = 0, \quad \bar{z} = (1 - z^2 R^2)/iz^2, \quad (47)$$

and the scaling parameter $q = (W/4)^{1/3}$. According to the definition of $z(\varepsilon)$ in Eq. (45), the solutions of Eqs. (46) and (47) are related to the boundary values of the DOS as

$$N(E) = (2q)^{-1} \text{Re } z, \quad N_{-1}(E) = (2q)^{-1} \text{Re } \bar{z}. \quad (48)$$

The results of computation of the DOS based on the numerical solution of the recurrences (34) and (35) and shown in Fig. 3, quantitatively confirm the results of our asymptotic analysis.

We note that at $eV < 2\Delta$ ($\Omega < 0$), the DOS in Eq. (48) exhibits a minigap at $eV - \Delta < E < \Delta$; within this region, the quantities R and \bar{R} are imaginary, and Eqs. (46) and (47) have purely imaginary roots $z(\varepsilon)$. This region corresponds to overlap of the gaps defined by unperturbed $N(E)$ and $N(E - eV)$, where the DOS is expected to be suppressed up to W^2 , which is equal to zero within our approximation.

VI. MULTIPARTICLE CURRENTS: THRESHOLDS

A. Two-particle current

The existence of the subgap states enables quasiparticles to overcome the energy gap at $eV < 2\Delta$ via two steps involving intermediate Andreev reflection at the energy $|E| < \Delta$. The population $n(E)$ of the intermediate state cannot be taken to be in equilibrium, because the subgap quasiparticles cannot access the equilibrium electrodes. In terms of the circuit approach, the node $k = 0$ is disconnected from the equilibrium source, and the subgap current flows through two resistances ρ_0 and ρ_1 (two-particle current), see Fig. 3(a). The corresponding partial currents are equal, $j_0 = j_1 = [n_F(E_1) - n_F(E_{-1})]/(\rho_0 + \rho_1)$, and their contribution to $I(V)$ is confined to the energy region $0 < E < eV - \Delta$ (a similar contribution at $\Delta < E < eV$ comes from j_0 and j_{-1}), which leads to the following expression for the two-particle current,

$$I_2 = \frac{4}{eR} \int_0^{eV - \Delta} \frac{dE}{\rho_0 + \rho_1}, \quad \Delta \leq eV < 2\Delta.$$

Within the SPT approximation for the subgap DOS function N , this is equivalent to equation

$$I_2 = \frac{4W}{eR} \int_0^{eV - \Delta} dE \left| \frac{\Delta}{\xi} \right|^a \frac{|E_1 E_{-1}|}{\xi_1 \xi_{-1}}, \quad (49)$$

where $\xi(E) = [(E + i0)^2 - \Delta^2]^{-1/2}$ according to Eq. (9b).

The two-particle current possesses a threshold at $eV = \Delta$. In the vicinity of the threshold, $eV = \Delta + \Omega$, $0 < \Omega \ll \Delta$, Eq. (49) simplifies, giving the current threshold value

$$I_2(\Delta) = \frac{2W\Delta}{eR} \int_0^\Omega \frac{dE}{\sqrt{\Omega^2 - E^2}} = \frac{\pi W\Delta}{eR} = 2WI_1(2\Delta). \quad (50)$$

The current increases with voltage and diverges at $eV = 2\Delta$ which is the result of the mentioned DOS singularity at $E = \Delta$.

B. Three-particle current

At $eV < \Delta$, a minigap opens in the DOS around the zero energy [see Fig. 3(b)], however, since the number of subgap resistors increases up to three: ρ_{-1} , ρ_0 and ρ_1 (three-particle current), the current across the minigap will persist as long as the network period exceeds the minigap size, $eV > 2(\Delta - eV)$,

i.e., at $eV > 2\Delta/3$. The corresponding partial currents are equal, $j_{-1} = j_0 = j_1 = [n_F(E_1) - n_F(E_{-2})]/(\rho_{-1} + \rho_0 + \rho_1)$, and their contribution to $I(V)$ is confined to the energy region $\Delta - eV < E < 2eV - \Delta$, which leads to the following expression for the three-particle current at zero temperature,

$$I_3 = \frac{3}{eR} \int_{\Delta - eV}^{2eV - \Delta} \frac{dE}{\rho_{-1} + \rho_0 + \rho_1}, \quad 2\Delta/3 \leq eV < \Delta. \quad (51)$$

Taking the subgap DOS functions N and N_{-1} in the SPT approximation, Eq. (37), we see that the central resistance is the largest, $\rho_0 \sim W^{-2}$, and dominates the net subgap resistance. Retaining only this resistance, we get

$$I_3 = \frac{3W^2}{eR} \int_{\Delta - eV}^{2eV - \Delta} dE \left| \frac{\Delta^2}{\xi \xi_{-1}} \right|^a \frac{|E_1 E_{-2}|}{\xi_1 \xi_{-2}}. \quad (52)$$

Calculating the integral in Eq. (52) in the vicinity of the threshold $eV = 2\Delta/3$, we obtain the threshold value

$$I_3(2\Delta/3) = \frac{3\pi\Delta W^2}{2eR} \left(\frac{9}{8}\right)^a \approx 2WI_2(\Delta). \quad (53)$$

While approaching the voltage value $eV = \Delta$, the current in Eq. (52) infinitely increases due to decreasing distance between the upper integration limit and the singular point $E = \Delta$.

C. Four-particle current

At $eV < 2\Delta/3$ the network period becomes smaller than the minigap, and the situation resembles the one encountered when the voltage decreased below 2Δ : we have to repeat the calculation cycle explained above, and to calculate the next (second-order) correction to the DOS $\sim W^2$. In the equation for the four-particle current [see Fig. 3(c)],

$$I_4 = \frac{8}{eR} \int_0^{2eV - \Delta} \frac{dE}{\rho_{-1} + \rho_0 + \rho_1 + \rho_2}, \quad \frac{\Delta}{2} \leq eV < \frac{2\Delta}{3}, \quad (54)$$

the largest resistances are $\rho_0 \sim \rho_1 \sim W^{-3}$, thus $\rho_{-1} \sim \rho_{-2} \sim W^{-1}$ can be neglected. The DOS functions $N_{\pm 1}$ which enter ρ_0 and ρ_1 can be obtained from the SPT equations (37) at $E = E_{\pm 1}$, in which small $N(E)$ in the rhs has to be neglected: $N_{\pm 1}(E) = W|\Delta/\xi|^a N_S(E_{\pm 2})$. To evaluate $N(E)$, we must perform next iteration step, by substituting these values of $N_{\pm 1}$ into the SPT equation (37) for $N(E)$. As the result, we obtain

$$I_4 = \frac{8W^3}{eR} \int_0^{2eV - \Delta} dE \left| \frac{\Delta^3}{\xi \xi_{-1} \xi_1} \right|^a \frac{|E_2 E_{-2}|}{\xi_2 \xi_{-2}}.$$

In the vicinity of the threshold $eV = \Delta/2$, this equation gives

$$I_4(\Delta/2) = \frac{2\pi\Delta W^3}{eR} \left(\frac{4}{3}\right)^a \approx 2WI_3(2\Delta/3). \quad (55)$$

While approaching the voltage value $eV = 2\Delta/3$, the four-particle current infinitely increases.

From these considerations we conclude that the evaluation of $2n$ - and $(2n + 1)$ -particle currents requires DOS recurrences of n th order. As long as the applied voltage decreases below Δ/n , a new minigap opens in the DOS (see discussion in Sec. V A), and the recurrent procedure should be repeated again.

VII. MULTIPARTICLE CURRENTS: LARGE VOLTAGE

It follows from the calculations in previous Sec. VI that the multiparticle currents have finite values in the vicinity of their thresholds, but they diverge at the next gap subharmonics: the two-particle current diverges at $eV = 2\Delta$, the three-particle current diverges at $eV = \Delta$, and so on. These divergences are caused by singularity of the SPT correction to the tunneling DOS at the point $E = \Delta$ which enters the integration region.

It is easy to see that the two-particle current persists also above the gap voltage, $eV > 2\Delta$: when the node n_0 is inside the gap, $|E| < \Delta$, the subgap circuit should consist of two resistors no matter how large the applied voltage is. Furthermore, since the singular point $E = \Delta$ always belongs to the integration region, the current will formally diverge at *all voltages* $eV > 2\Delta$; generally, the n -particle current ($n > 1$) taken in the SPT approximation diverges at all voltages above $eV = 2\Delta/(n-1)$. This catastrophe is known since the pioneering calculations of the two-particle current within the tunneling Hamiltonian model.¹ It implies in fact that the currents have nonanalytical dependencies on the tunneling parameter W at large voltages (cf. Ref. 2). These divergences can be eliminated by using the improved perturbation expansion of Sec. VB.

We also note that the three-particle current disappears at large enough voltage, in contrast to the two-particle current which persists at all voltages. This is obvious from the circuit geometry in Fig. 3: as soon as eV exceeds 2Δ , the network period becomes larger than the energy gap, therefore the subgap circuit may involve no more than two resistors. This is relevant for all n -particle currents with $n > 2$ which persist only within the voltage intervals $2\Delta/n < eV < 2\Delta/(n-2)$ and abruptly disappear at larger voltages (see Fig. 4).

A. Two-particle current at $eV \geq 2\Delta$

The two-particle current at $eV > 2\Delta$ is given by equation

$$I_2 = \frac{4}{eR} \int_0^\Delta \frac{dE}{\rho_0 + \rho_1} = \frac{4}{eR} \int_0^\Delta \frac{NdE}{N_1^{-1} + N_{-1}^{-1}}. \quad (56)$$

To evaluate the integral, we use the IPT equations (39)–(42) to calculate $N(E)$, while the functions $N_{\pm 1}$ are taken in the BCS form. Furthermore all the smooth functions can be approximated with their values at the singular point $E = \Delta$,

$$g(eV) = (1/2) \sum_{k=\pm 1} N_S(\Delta + keV), \quad (57a)$$

$$N_1^{-1} + N_{-1}^{-1} = \sum_{k=\pm 1} N_S^{-1}(\Delta + keV) \equiv h^{-1}(eV). \quad (57b)$$

As the result, we obtain

$$I_2 = \frac{2\Delta}{eR} C_1 p(eV) h(eV) \sim W^b, \quad (58)$$

$$C_1 = \int_0^\infty d\varepsilon \operatorname{Im} z(\varepsilon) = \begin{cases} 9\sqrt{3}/4, & \text{1D junction,} \\ \sqrt{2}, & \text{planar junction.} \end{cases}$$

where $p(eV)$ is given by Eq. (39) or Eq. (41) depending on the junction geometry. As it was expected, the two-particle

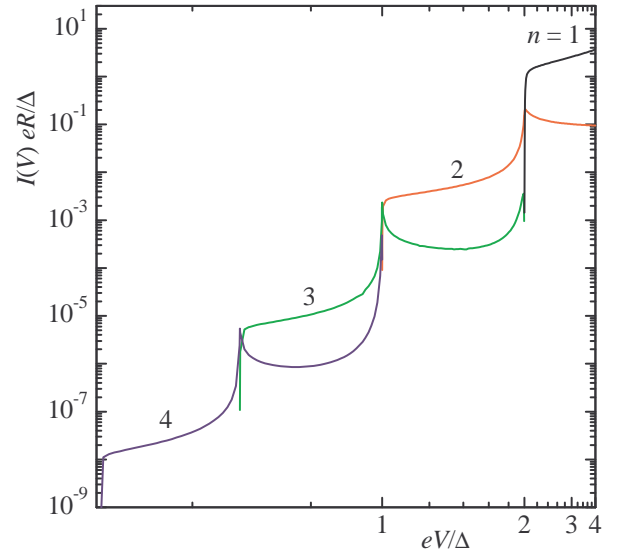


FIG. 4: (Color online) Multiparticle currents in planar junction numerically computed for the tunneling parameter $W = 10^{-3}$.

current in this region is given by a nonanalytical expression with respect to W , and it is larger than the current value at smaller voltages $eV < \Delta$.

Important property of the tunneling IVC is the excess current I_{exc} , i.e., voltage-independent deviation of the total current from the ohmic IVC at large voltage $eV \gg \Delta$. The excess current is readily evaluated by considering this limit in Eqs. (57) and (58),

$$I_{exc} = \frac{\Delta}{eR} W^b \times \begin{cases} 6.19, & \text{1D junction,} \\ 2.83, & \text{planar junction.} \end{cases} \quad (59)$$

Our analysis is not complete yet because the current in Eq. (58) grows infinitely when the voltage approaches 2Δ . The divergence, caused by singular behavior of the term N_{-1} in Eq. (57a), can be eliminated by using more accurate approximation of Eqs. (45)–(48) for $N(E)$. Neglecting a non-singular term N_1 in the denominator in Eq. (56),

$$I_2 = \frac{4}{eR} \int_0^\Delta dE \frac{NN_1 N_{-1}}{N_1 + N_{-1}} \approx \frac{4}{eR} \int_0^\Delta dE NN_1,$$

and approximating N_1 with $N(3\Delta) = 3/2\sqrt{2}$, we obtain

$$I_2(2\Delta) = \frac{6q\Delta}{\sqrt{2}eR} \int_0^\infty d\varepsilon \operatorname{Re} z(-\varepsilon) \approx \frac{\Delta}{eR} W^{1/a} \times \begin{cases} 2.32, & \text{1D junction;} \\ 2.50, & \text{planar junction;} \end{cases} \quad (60)$$

Thus we see that the two-particle current possesses a pronounced peak at $eV = 2\Delta$, which exceeds not only the current threshold value, but also the large excess current, see Fig. 4.

B. Three-particle current at $eV \geq \Delta$

The three-particle current at $eV \geq \Delta$ is given by Eq. (51), in which the integration limits should assume different values, $eV - \Delta < E < \Delta$. Using the symmetry relation $N(E) =$

$N(-E)$, we reduce the integration region to the interval $eV/2 < E < \Delta$, containing only one dangerous point $E = \Delta$,

$$I_3 = \frac{6}{eR} \int_{eV/2}^{\Delta} \frac{dE}{\rho_{-1} + \rho_0 + \rho_1}. \quad (61)$$

At this point, all terms in the denominator turn to zero being calculated within the SPT approximation. To eliminate the divergence, we apply the IPT approach, Eqs. (42) and (39), to calculate N , which then assumes a finite value $N \sim W^{-b}$ at the singular point. In the present case the function g defined in Eq. (38) has a complex-valued form $g(eV) = |g|e^{i\varphi}$ because the energy E_{-1} in this equation occurs inside the gap:

$$|g| = \frac{\Delta^{3/2}}{\sqrt{eV[4\Delta^2 - (eV)^2]}}, \quad \tan \varphi = \frac{eV - \Delta}{eV + \Delta} \sqrt{\frac{2\Delta + eV}{2\Delta - eV}}. \quad (62)$$

Thus the scaling factor p in Eqs. (39a), (41), and (42) is to be defined through the modulus of g , while the phase factor will remain in the equation for z in 1D geometry,

$$z^3 \exp(2i\varphi) + (z\sqrt{\varepsilon} - 1)^2 = 0, \quad (63)$$

and in the expression for z for planar geometry,

$$z = [\varepsilon - i \exp(i\varphi)]^{-1/2}. \quad (64)$$

Therefore the normalized spectral function becomes dependent on eV . The function N_{-1} can then be evaluated from the SPT approximation, keeping only large quantity N in the rhs,

$$N_{-1} = W|\Delta/\xi_{-1}|^a N. \quad (65)$$

At the singular point, $N_{-1} \sim W^{1-b}$. The other relevant functions N_1 and N_{-2} can be taken in the BCS form, thus having magnitudes ~ 1 . The values of the subgap resistances are $\rho_{-1} \sim W^{b-1} \gg \rho_0 \sim W^{2b-1}$ and $\rho_1 \sim W^b$; retaining only the largest resistance ρ_{-1} in Eq. (61), we get

$$I_3 = \frac{6}{eR} \int_{eV/2}^{\Delta} dE N_{-1} N_{-2} = \frac{6Wp\Delta}{eR} N_{-2} \left| \frac{\Delta}{\xi_{-1}} \right|^a C_2 \sim W^{1+b}, \quad (66)$$

$$C_2(eV) = \int_0^{\infty} d\varepsilon \operatorname{Im} z(\varepsilon, eV)$$

[for planar model, $C_2(eV) = 2\cos(\varphi/2 + \pi/4)$]. Here the functions N_{-2} and ξ_{-1} should be taken at the point $E = \Delta$. This expression diverges at $eV = \Delta$ and $eV = 2\Delta$. In fact, the current has a finite peak value at $eV = \Delta$; another peak appears slightly below $eV = 2\Delta$, because the current turns to zero at $eV = 2\Delta$, as follows from Eq. (61) (see Fig. 4).

To evaluate the current peak value at $eV = \Delta$, we reduce the integration to the interval $\Delta/2 < E < \Delta$. Since now N_{-2} is also large at the singular point, we should keep it in Eq. (65) together with N , i.e., $N_{-1} = W(N + N_{-2})$. Both the functions N and N_{-2} are to be evaluated using the IPT scheme, Eqs. (38)–(42). This leads to expressions $N = (2p)^{-1} \operatorname{Im} z_+(\varepsilon)$ and $N_{-2} = (2p)^{-1} \operatorname{Re} z_-(\varepsilon)$, where the spectral functions z_{\pm} are given by the solutions of algebraic equations

$$z_+^3 + (z_+ \sqrt{\varepsilon} - 1)^2 = 0, \quad iz_-^3 + (z_- \sqrt{\varepsilon} - 1)^2 = 0 \quad (67)$$

in the case of 1D junction, or by explicit expressions

$$z_{\pm} = (\varepsilon \mp i)^{-1/2} \quad (68)$$

in the case of a planar junction; the scaling parameter p is $(W^2/6)^{1/3}$ and $(W/\sqrt{3})^{1/2}$, respectively. Then the largest resistances are $\rho_0 \sim \rho_{-1} \sim W^{2b-1}$, while the resistance $\rho_1 \sim W^b$ can be neglected. As the result, we obtain

$$I_3(\Delta) = \frac{6W}{eR} \int_{\Delta/2}^{\Delta} dE N N_{-2} = \frac{3W\Delta}{eR} \int_0^{\infty} d\varepsilon \operatorname{Im} z_+ \operatorname{Re} z_- \\ = \frac{W\Delta}{eR} \times \begin{cases} 3.16, & \text{1D junction;} \\ 3\pi/4, & \text{planar junction.} \end{cases} \quad (69)$$

Analysis of the current behavior near $eV = 2\Delta$, which we do not present here, gives the following estimate for the current peak value: $I_{3max} \sim W^{4/5} \Delta / eR$ for the 1D junction and $I_{3max} \sim W\Delta / eR$ for the planar junction.

C. Four-particle current at $eV \geq 2\Delta/3$

The four-particle current at $eV \geq 2\Delta/3$ is given by Eq. (54), in which the upper integration limit is replaced by the value $\Delta - eV$, representing a singular point of the integrand. The functions N and N_{-1} are calculated from the SPT equations (37), neglecting small subgap values of N_{-1} and N in the rhs,

$$N = W|\Delta/\xi|^a N_1, \quad N_{-1} = W|\Delta/\xi_{-1}|^a N_{-2}. \quad (70)$$

Within the voltage interval $2\Delta/3 < eV < \Delta$ (excluding specific points $2\Delta/3$ and Δ) we can apply the BCS approximation for the functions $N_{\pm 2}$. However, the function N_1 should be calculated by means of the IPT approach, Eqs. (38)–(42), as soon as the energy E_1 hits the singular point. The resulting equations for N_1 coincide with that for N in previous Section [Eqs. (62)–(64); in present case, $\tan \varphi$ is negative]. Thus, at the singular point, $N_1 \sim W^{-b}$, $N_0 \sim W^{1-b}$, $N_{-1} \sim W$, and $N_{\pm 2} \sim 1$. Therefore the resistance $\rho_0 \sim W^{b-2}$ dominates, while $\rho_{-1} \sim W^{-1}$, $\rho_1 \sim W^{2b-1}$, and $\rho_2 \sim W^b$ can be neglected.

The result of calculation of the integral over energy reads

$$I_4 = \frac{8\Delta W^2}{eR} C_2(eV) p(eV) \left| \frac{\Delta^2}{\xi \xi_{-1}} \right|^a N_{-2} \sim W^{2+b}, \quad (71)$$

where the functions ξ , ξ_{-1} , and N_{-2} are taken at $E = \Delta - eV$. This expression diverges at the points $eV = 2\Delta/3$ and $eV = \Delta$, where the IPT should be applied.

Let us evaluate the current peak value at $eV = 2\Delta/3$. Since both the BCS and SPT approximations for N_{-2} diverge at this point, we evaluate the functions N_1 and N_{-2} in the rhs of Eqs. (70) using the IPT equations (38)–(42),

$$N_1(E) = (2p)^{-1} \operatorname{Im} z_+(\varepsilon), \quad N_{-2}(E) = (2p)^{-1} \operatorname{Re} z_-(\varepsilon). \quad (72)$$

Here the functions z_{\pm} obey the equations (67) or (68) modified by the phase factors similar to Eqs. (63) and (64). In this case, $\tan \varphi = -\sqrt{2}/5$, and the scaling factor is $p = (3/4)(W^2/2)^{1/3}$ for 1D junctions and $p = (3W\sqrt{3}/8)^{1/2}$ for planar junctions.

The corresponding estimates for the DOS functions are $N_1 \sim N_{-2} \sim W^{-b}$, $N \sim N_{-1} \sim W^{1-b}$, while $N_2 \sim 1$ can be taken in BCS approximation. Therefore the largest resistance is $\rho_0 \sim W^{2b-2}$, while $\rho_{-1} \sim \rho_1 \sim W^{2b-1}$ and $\rho_2 \sim W^b$ can be neglected. As the result for the current we get

$$\begin{aligned} I_4(2\Delta/3) &= \frac{4\Delta W^2}{eR} \left(\frac{9}{8}\right)^a \int_0^\infty d\varepsilon \text{Im} z_+ \text{Re} z_- \\ &= \frac{\Delta W^2}{eR} \times \begin{cases} 6.63, & \text{1D junction;} \\ 5.26, & \text{planar junction.} \end{cases} \end{aligned} \quad (73)$$

Analysis of the current behavior near $eV = \Delta$ gives the estimate $I_{4max} \sim W\Delta/eR$ for the current peak value.

D. Subharmonic gap structure

Extending the results of our analysis over all high-order multiparticle currents, we conclude that they exhibit a similar pattern of the voltage dependence (see Fig. 4): n -particle current appears above the threshold $eV = 2\Delta/n$, having roughly the value $I_n \sim (2W)^{n-1}I_1$, then increases and shows dramatic peak while approaching $eV = 2\Delta/(n-1)$; then it remains anomalously large within the voltage interval $2\Delta/(n-1) < eV < 2\Delta/(n-2)$, and eventually disappears at $eV = 2\Delta/(n-2)$, showing another strong peak at slightly smaller voltage.

The net tunnel current consists of the sum of the n -particle currents, and therefore exhibits pronounced step-like structure on the IVC with steps at the gap subharmonics $eV = 2\Delta/n$, as shown in Fig. 5 obtained by numerical calculation at $T = 0$. The peaks of the multiparticle currents with numbers $n+1$ and $n+2$ produce small spikes at the n th threshold with $n > 1$; the example of such spike is presented in the inset of Fig. 5. The numerical procedure involves solving the set of recurrences (34) or (35) for the functions θ_k which correspond to the sub-gap energies, $|E_k| \leq \Delta$ ($-N_- < k < N_+$); the non-singular terms in these equations are replaced with the BCS values. For the voltage values equal to the gap subharmonics one more equation is to be added as explained in the previous sections. We note that the results for the 1D and planar geometries differ insignificantly; in logarithmic scale, the difference can be detected only in the immediate vicinity of the peaks.

Such a picture is quite similar to the tunneling SGS in quantum point contacts,^{2,10,12} and the resulting IVC is found to be very close to the result for a point contact with the effective transparency $D_{eff} = 4W$.

VIII. EFFECT OF FIRST HARMONICS

In this Section we evaluate the effect of higher harmonics on the dc subgap current. We restrict our calculation to first order in the tunneling parameter W thus taking into account only two first harmonics $m = \pm 1$. The main conclusion of our calculation will be that including harmonics produces just insignificant quantitative changes, while major qualitative properties of the SGS, positions and scaling of the multiparticle current steps will not change.

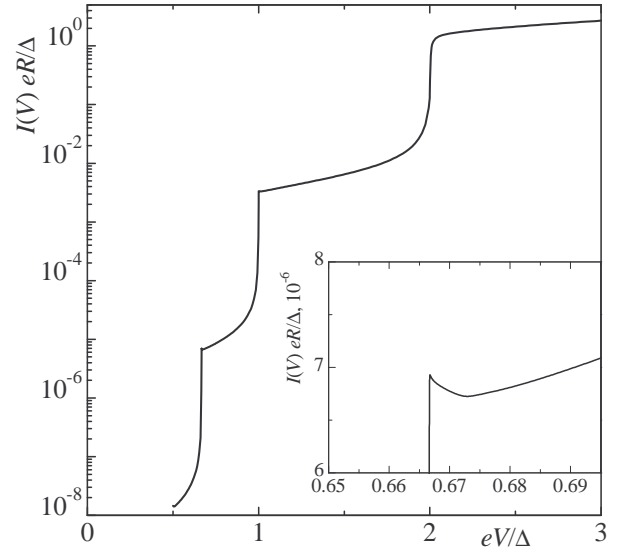


FIG. 5: I - V characteristic with tunneling SGS for planar junction computed numerically for the tunneling parameter $W = 10^{-3}$. The inset shows a spike of the IVC near the threshold of the three-particle current, $eV \approx 2\Delta/3$.

We start with a general equation (13) for the dc current, and evaluate an additional contribution due to the first harmonics in the Keldysh and Green's functions,

$$\begin{aligned} \delta I &= \frac{1}{32eR} \int_{-\infty}^{\infty} dE \text{Tr} \sum_{m=\pm 1} m \sigma_z [\hat{h}(E, 0) \hat{G}^K(E, m) \\ &\quad + \hat{h}(E, -m) \hat{G}^K(E, 0)] \\ &= \frac{i}{4eR} \int_{-\infty}^{\infty} dE \sum_{m=\pm 1} m [v_y(E, m) \text{Im} v + v \text{Im} v_y(E, m)]. \end{aligned} \quad (74)$$

Only *off-diagonal* parts of matrices \hat{h} and \hat{G}_K enter this equation. We remind that Eq. (74) is written in terms of the boundary values of the Green's and Keldysh functions at the junction. Here and below we will use the subscripts (x, y, z) to indicate the corresponding matrix components of the first harmonics of the Green's and Keldysh functions, while the zero harmonic of the matrix components will be used as before without such subscripts, u and v . Thus $v[V]$ in Eq. (74) indicates y -component of $\hat{g}(E, 0)$ [$\hat{G}^K(E, 0)$], and $v_y(E, \pm 1)$ [$V_y(E, \pm 1)$] indicates the y -component of $\hat{g}(E, \pm 1)$ [$\hat{G}^K(E, \pm 1)$].

A. Perturbation theory for the Green's functions

To evaluate the current in Eq. (74), one needs to find the y -component in the Green's function expansion over the Pauli matrices, $\hat{g}(z, E, m) = \sigma_z u_z + i\sigma_y v_y + \sigma_x v_x + w$. In what follows, we will focus on the case of 1D junction. Considering the Usadel equation (5) to first order in W , we arrive at the equation for the functions $v_y(z, E, m)$ and $u_z(z, E, m)$,

$$meV u_z(z) = 2i\Delta [u_m u_z''(z) - v_m v_y''(z)]. \quad (75)$$

In this and following derivations we neglect small deviation of the functions u and v from the BCS form Eq. (9b). We

will use the following convention to avoid cumbersome notations: the zero harmonics with shifted energy arguments $E + meV$ will be denoted with the subscript m , as before, e.g., $u_m \equiv u(E + meV, 0)$, while the first harmonics will be denoted with an argument, e.g., $v_y(E, \pm 1)$; the absence of the explicit argument would mean the relevance to the both harmonics $m = \pm 1$. Also, the spatial dependence will be explicitly indicated when its absence may lead to confusions, otherwise the function will be assumed to be taken at the boundary $z = -0$.

The function u_z can be excluded from Eq. (75) by virtue of the normalization condition $(u_1 + u_{-1})u_z(E, m) = (v_1 + v_{-1})v_y$. The boundary condition for Eq. (75) results from Eq. (7a) and determines the boundary value of first derivative,

$$v'_y|_{z=-0} = (W/2)v(1 + u_1u_{-1} + v_1v_{-1}). \quad (76)$$

Solving Eq. (75), $v_y(z) = v_y \exp(k_1 z)$ ($z < 0$), we establish the following relation at the boundary,

$$v_y(E, m) = k_1^{-1} v'_y(E, m), \quad k_1^2 = (\xi_1 + \xi_{-1})/2i\Delta. \quad (77)$$

Equations (76) and (77) allow us to express the first harmonics $v_y(E, m)$ through known zero harmonics u and v , and to establish the relation $v_y(E, 1) = v_y(E, -1)$ which implies that the second term in Eq. (74) turns to zero.

B. Perturbation theory for Keldysh function

To calculate the harmonics of the Keldysh function, it is convenient to separate the contributions of the Green's function harmonics and the harmonics of the distribution function,

$$\begin{aligned} \hat{G}^K(E, m) &= \delta \hat{G}^K(E, m) + \hat{G}^K(E, m), \\ \delta \hat{G}^K(E, m) &= \hat{g}^R(E, m)f_{-m} - f_m \hat{g}^A(E, m), \\ \hat{G}^K(E, m) &= \hat{g}_m^R f(E, m) - f(E, m) \hat{g}_{-m}^A. \end{aligned} \quad (78)$$

In Eqs. (78) we used the rule Eq. (11) for the convolutions valid for the first harmonics, $(A \circ B)(E, m) = A(E, m)B_{-m} + A_m B(E, m)$, which allows us to write the equation for the function \hat{G}^K following from Eqs. (6a) and (7) in a symbolic form

$$[\hat{H}, \circ \hat{G}^K] = 2i\Delta \partial_x (\hat{g}^R \circ \partial_x \hat{G}^K + \hat{G}^K \circ \partial_x \hat{g}^A), \quad (79)$$

where small gradient of the distribution function, $\partial_x f \sim L^{-1}$, has been neglected. The boundary condition to Eq. (79) reads

$$\begin{aligned} \hat{g}^R \circ \partial_x \hat{G}^K &= W(\hat{g}^R \circ \hat{\mathcal{F}} - \hat{\mathcal{F}} \circ \hat{g}^A), \\ \hat{\mathcal{F}} &= \overline{\hat{g}^R} \circ (\overline{f} - f) - (\overline{f} - f) \circ \overline{\hat{g}^A}. \end{aligned} \quad (80)$$

According to Eq. (74), we are interested in the y -component in the expansion $\hat{G}^K = \sigma_z \mathcal{U}_z + i\sigma_y \mathcal{V}_y + \sigma_x \mathcal{V}_x + \mathcal{W}$. The equation for this component is similar to Eq. (75), $meV \mathcal{U}_z = 2i\Delta [u_m \mathcal{U}_z'' - v_m \mathcal{V}_y'']$. The normalization condition Eq. (6b) gives the relation $(v_m - v_{-m}^*) \mathcal{U}_z(E, m) = (u_m - u_{-m}^*) \mathcal{V}_y(E, m)$ which allows us to obtain a closed differential equation for \mathcal{V}_y . Solution of this equation at $z < 0$ has the form $\mathcal{V}_y(z) = \mathcal{V}_y \exp(q_1 z)$, giving the following relation at the boundary,

$$\mathcal{V}_y(E, m) = q_1^{-1} \mathcal{V}'_y(E, m), \quad q_1^2 = (\xi_1 - \xi_{-1}^*)/2i\Delta, \quad (81)$$

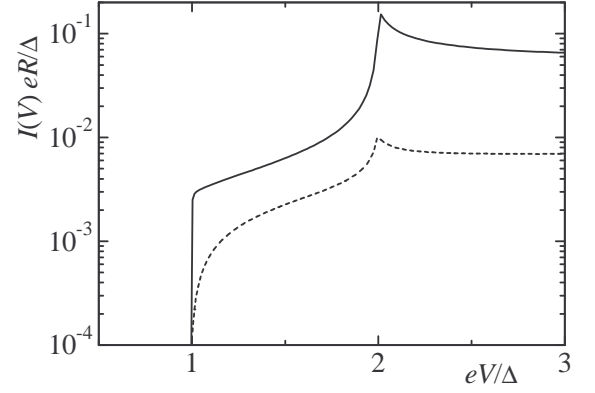


FIG. 6: Current of first harmonics (dashed line) compared to the two-particle current (solid line), for the tunneling parameter $W = 10^{-3}$.

where the quantity \mathcal{V}_y is to be determined from the boundary condition Eq. (80),

$$\mathcal{V}'_y|_{z=-0} = W(1 - u_m u_{-m}^* - v_m v_{-m}^*) \Phi(E, m), \quad (82)$$

$$\Phi(E, m) = M \left(f - \frac{1}{2} \sum_{k=\pm 1} f_k \right) + \frac{i}{2} \text{sgn}(m) M_S \sum_{k=\pm 1} k f_k,$$

where $M = \text{Re } v$ [see Eq. (15)], and $M_S = \text{Im } v$. At $T = 0$,

$$\Phi(E, m) = \Theta[(eV)^2 - E^2] [\text{sgn}(E)M + i \text{sgn}(m)M_S].$$

C. Current of first harmonics

The function $\mathcal{V}_y(E, m)$, which determines the current in Eq. (74), is now expressed, according to Eq. (78), through the quantities calculated in Eqs. (76)–(77) and Eqs. (81)–(82), $\mathcal{V}_y(E, m) = v_y f_{-m} + v_y^* f_m + \mathcal{V}_y$. Collecting all these equations and substituting them into Eq. (74), we get

$$\begin{aligned} \delta I &= \frac{W}{4eR} \int_{-\infty}^{\infty} dE \text{Im } v \left\{ (f_1 - f_{-1}) \text{Im} \left(\frac{v}{k_1} \cosh^2 \frac{\chi}{2} \right) \right. \\ &\quad \left. + \text{Im} \left[\frac{v}{q_1} (f - f_{-1}) + \frac{v^*}{q_1} (f - f_1) \sinh^2 \frac{\tilde{\chi}}{2} \right] \right\}, \end{aligned}$$

where $\chi = \theta_1 + \theta_{-1}$ and $\tilde{\chi} = \theta_1 + \theta_{-1}^*$. At $T = 0$, this equation reduces to the following form:

$$\delta I = \frac{2W}{eR} \int_0^{eV} dE \text{Im } v \text{Im} \left(\frac{v}{k_1} \cosh^2 \frac{\chi}{2} + \frac{v}{q_1} \sinh^2 \frac{\tilde{\chi}}{2} \right). \quad (83)$$

We note that in the resulting Eq. (83) all the spectral functions are retarded and assume the BCS form. Similar considerations in the case of a planar junction result in replacements $q_1 \rightarrow q_1^2$ and $k_1 \rightarrow k_1^2$ in the rhs of Eq. (83). Noting also that at $eV < \Delta$ the energy E_{-1} in Eq. (83) appears in the subgap region, where $\theta_{-1}^* = \theta_{-1} + \pi i$ and $\xi_{-1}^* = -\xi_{-1}$, we find that δI turns to zero at $eV < \Delta$, similar to I_2 . Numerical calculations show that the contribution of the first harmonics to the net dc current does not exceed 30% (see Fig. 6). From this we conclude that the adopted quasi-static approximation, where the nonzero harmonics are neglected, gives a relatively good approximation to a complete solution.

Acknowledgments

The support from the SSF-OXIDE Consortium, the Swedish Research Council (VR), and the Royal Academy of Sci-

ence (KVA) is gratefully acknowledged.

-
- ¹ J. R. Schrieffer and J. W. Wilkins, Phys. Rev. Lett. **10**, 17 (1963); J. W. Wilkins in *Tunneling Phenomena in Solids* (Plenum, NY, 1963), p. 333; L. E. Hasselberg, M. T. Levinsen, and M. R. Samuelsen, Phys. Rev. B **9**, 3757 (1974).
- ² E. N. Bratus', V. S. Shumeiko, and G. Wendin, Phys. Rev. Lett. **74**, 2110 (1995).
- ³ T. M. Klapwijk, G. E. Blonder, and M. Tinkham, Physica B+C, **109-110**, 1657 (1982).
- ⁴ D. Averin and A. Bardas, Phys. Rev. Lett. **75**, 1831 (1995).
- ⁵ J. C. Cuevas, A. Martin-Rodero, and A. Levy Yeyati, Phys. Rev. B **54**, 7366 (1996).
- ⁶ B. N. Taylor and E. Burstein, Phys. Rev. Lett. **10**, 14 (1963).
- ⁷ R. Cristiano, L. Frunzio, R. Monaco, C. Nappi, and S. Pagano, Phys. Rev. B **49**, 429 (1994).
- ⁸ M. A. Gubrud, M. Ejtnaes, A. J. Berclay, R. C. Ramos, Jr., J. R. Anderson, A. J. Dragt, C. J. Lobb, and F. C. Wellstood, IEEE Trans. Appl. Supercond. **11**, 1002 (2001).
- ⁹ K. M. Lang, S. Nam, J. Aumentado, C. Urbina, and J. M. Martinis, IEEE Trans. Appl. Supercond. **13**, 989 (2003); S. Oh, K. Ciccal, R. McDermott, K. B. Cooper, K. D. Osborn, R. W. Simmonds, M. Steffen, J. M. Martinis, and D. P. Pappas, Supercond. Sci. Techn. **18**, 1396 (2005).
- ¹⁰ N. van der Post, E. T. Peters, I. K. Yanson, and J. M. van Ruitenbeek, Phys. Rev. Lett. **73**, 2611 (1994).
- ¹¹ E. Scheer, P. Joyez, D. Esteve, C. Urbina, and M. H. Devoret, Phys. Rev. Lett. **78**, 3535 (1997).
- ¹² B. Ludoph, N. van der Post, E. N. Bratus', E. V. Bezuglyi, V. S. Shumeiko, G. Wendin, and J. M. van Ruitenbeek, Phys. Rev. B **61**, 8561 (2000).
- ¹³ A. W. Kleinsasser, R. E. Miller, W. H. Mallison and G. B. Arnold, Phys. Rev. Lett. **72**, 1738 (1994).
- ¹⁴ E. V. Bezuglyi, A. S. Vasenko, E. N. Bratus', V. S. Shumeiko, and G. Wendin, Phys. Rev. B **73**, 220506(R) (2006).
- ¹⁵ A. I. Larkin and Yu. N. Ovchinnikov, in *Nonequilibrium Superconductivity*, edited by D. N. Langenberg and A. I. Larkin (Elsevier, Amsterdam, 1986).
- ¹⁶ W. Belzig, F. K. Wilhelm, C. Bruder, G. Schön, and A. D. Zaikin, Superlatt. Microstruct. **25**, 1251 (1999).
- ¹⁷ M. Eschrig, Phys. Rev. B **61**, 9061 (2000).
- ¹⁸ E. V. Bezuglyi, E. N. Bratus', V. S. Shumeiko, G. Wendin, and H. Takayanagi, Phys. Rev. B **62**, 14439 (2000).
- ¹⁹ J. C. Cuevas, J. Hammer, J. Kopu, J. K. Viljas, and M. Eschrig, Phys. Rev. B **73**, 184505 (2006).
- ²⁰ Yu. V. Nazarov, Superlatt. Microstruct. **25**, 1221 (1999).
- ²¹ C. W. J. Beenakker, Phys. Rev. Lett. **67**, 3836 (1991); *ibid.* **68**, 1442 (1992).
- ²² A. Bardas and D. Averin, Phys. Rev. B **56**, R8518 (1997).
- ²³ C. W. J. Beenakker, B. Rejaei, and J. A. Melsen, Phys. Rev. Lett. **72**, 2470 (1994).
- ²⁴ A. F. Volkov, Physica B **203**, 267 (1994).
- ²⁵ N. R. Werthamer, Phys. Rev. **147**, 255 (1966).
- ²⁶ A. I. Larkin and Yu. N. Ovchinnikov, Sov. Phys. JETP **24**, 1035 (1967).
- ²⁷ M. Yu. Kupriyanov, JETP Lett. **56**, 399 (1992); E. V. Bezuglyi, E. N. Bratus', and V. P. Galaiko, Low Temp. Phys. **25**, 167 (1999); A. V. Galaktionov and Chang-Mo Ryu, J. Phys.: Condens. Matter **12**, 1351 (2000).
- ²⁸ M. Yu. Kupriyanov and V. F. Lukichev, Sov. Phys. JETP **67**, 1163 (1988).
- ²⁹ Yu. N. Ovchinnikov, Sov. Phys. JETP **32**, 72 (1971).
- ³⁰ S. N. Artemenko, A. F. Volkov, and A. V. Zaitsev, Sov. Phys. JETP **49**, 924 (1979).
- ³¹ Similar approach is used in the theory of ballistic point contacts,^{2,5} where the Josephson coupling is described by an effective time-dependent matching condition for the gauge-transformed Bogolyubov-de Gennes equations in the leads.
- ³² E. V. Bezuglyi, A. S. Vasenko, V. S. Shumeiko, and G. Wendin, Phys. Rev. B **72**, 014501 (2005).
- ³³ E. V. Bezuglyi and V. Vinokur, Phys. Rev. Lett. **91**, 137002 (2003).